

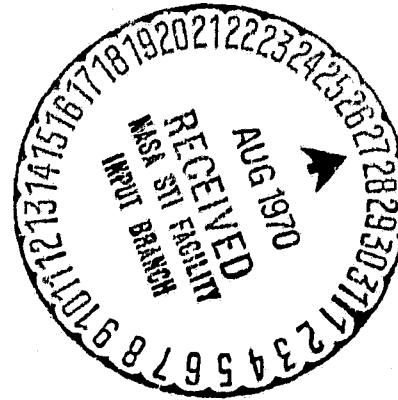
## **General Disclaimer**

### **One or more of the Following Statements may affect this Document**

- This document has been reproduced from the best copy furnished by the organizational source. It is being released in the interest of making available as much information as possible.
- This document may contain data, which exceeds the sheet parameters. It was furnished in this condition by the organizational source and is the best copy available.
- This document may contain tone-on-tone or color graphs, charts and/or pictures, which have been reproduced in black and white.
- This document is paginated as submitted by the original source.
- Portions of this document are not fully legible due to the historical nature of some of the material. However, it is the best reproduction available from the original submission.

## NASA PROGRAM APOLLO WORKING PAPER NO. 1178

## DYNAMIC SPACECRAFT SIMULATION



FACILITY FORM 602

N70-35725

(ACCESSION NUMBER)

24

(PAGES)

TMX 65846

(NASA CR OR TMX OR AD NUMBER)

(THRU)

(CODE)

07

(CATEGORY)



NATIONAL AERONAUTICS AND SPACE ADMINISTRATION

MANNED SPACECRAFT CENTER

HOUSTON, TEXAS

JULY 28, 1965

NASA PROGRAM APOLLO WORKING PAPER NO. 1178

DYNAMIC SPACECRAFT SIMULATION

Prepared by: Jack W. Seyl  
J. W. Seyl  
AST, Systems Engineering and Test Branch  
Information Systems Division

Jan W. Martin  
J. W. Martin  
AST, Systems Analysis Branch  
Information Systems Division

Authorized for Distribution:

Warren Gillespie, Jr  
for Maxime A. Feget  
Assistant Director for Engineering and Development

NATIONAL AERONAUTICS AND SPACE ADMINISTRATION

MANNED SPACECRAFT CENTER

HOUSTON, TEXAS

JULY 28, 1965

## CONTENTS

Section	Page
SUMMARY . . . . .	1
INTRODUCTION . . . . .	1
PURPOSE . . . . .	2
SIGNAL CHARACTERISTICS . . . . .	2
SIMULATION TECHNIQUE . . . . .	6
RF Doppler Simulation . . . . .	7
Code Doppler Simulation . . . . .	9
Range Time Delay . . . . .	15
CONCLUSIONS . . . . .	18
REFERENCES . . . . .	19
APPENDIX . . . . .	20



## SUMMARY

Realistic simulation of doppler and range time delay for the USB ranging system can be accomplished. This paper describes a technique using frequency translation for simulation of RF and clock doppler, and digital delay of the subcode components for range time delay simulation. The resulting test signals are shown to possess the characteristics which would actually be present due to the doppler phenomenon and range time delay. The techniques described deal mainly with simulation of signals applicable to the ranging subsystem. However, extension of these techniques to the up-data, PCM telemetry, T.V., voice (up and down) and emergency voice signals seems quite feasible. This would involve shifting or translation of the individual subcarriers. In most cases, however, telemetry and up-data spectrum distortion could also be simulated by translation of the data bit rate.

There are several possible approaches to this simulation problem; however, the techniques described here are felt to be the most practical for providing a truly realistic simulation of the doppler phenomenon.

## INTRODUCTION

During the Electronic Systems Test Program it is necessary to verify, with a high degree of confidence, that the Apollo Systems (remote-site, spacecraft, and IMCC) will be compatible during operational missions. To provide this high degree of confidence, characteristics of test signals must be made as realistic as possible. Ideally, this means that the operation of all systems and their respective signal characteristics will be identical to the conditions encountered during an actual mission. To this end, an investigation of the requirements for simulation of a dynamic spacecraft was undertaken. Three effects are to be considered:

1. Doppler phenomenon,
2. Range time delay,
3. Spacecraft position (angle tracking).

Only the first two effects (doppler and range delay) will be discussed. The requirements for simulation of spacecraft position will be investigated separately and presented at a later date.

## PURPOSE

The purpose of this paper is to describe the signal characteristics due to doppler and range delay, and to indicate one possible approach to simulating these effects. It is not intended that this paper constitute a final design for mechanization of the required simulation equipment.

## SIGNAL CHARACTERISTICS

The effects due to the relative motion between the spacecraft and ground station, which is essentially a doppler frequency shift, can best be visualized by illustration. For simplicity let us assume that the spacecraft is moving directly away from the ground station with a constant velocity  $v_s$ . Let the S-band signal be  $f_t$  and the transmitter clock associated with the range code be  $f_c$ . Since the various subcode elements in the range code are periodic every 11, 31, 63, and 127 microseconds, and the clock is a 500 kc square wave, the elements produce

spectral components at frequencies of  $\frac{nf_c}{11}$ ,  $\frac{nf_c}{31}$ ,  $\frac{nf_c}{63}$ , and  $\frac{nf_c}{127}$ ,

respectively, where  $n$  is an odd integer ( $n = 1, 3, 5, 7$ )<sup>1</sup>.

Figure 1 shows the transmitted signal power spectrum resulting from modulating the S-band carrier with the range code. Note that only the  $x$  subcode component and its harmonics are shown; again this is for simplicity, realizing that components are present due to the other subcode elements. This spectrum is transmitted to the spacecraft, where it is coherently detected, multiplied by a constant  $K = \frac{240}{221}$ , and retransmitted to the ground station. Since the constant  $K$  merely introduces an additional multiplying constant into the doppler equations, it is neglected in the following discussion. The received signal thus contains the two-way doppler shift. The received spectrum is shown in figure 2. It is seen that the S-band frequency  $f_t$  has been shifted in frequency by an

amount,  $f_d = \frac{2v_s f_t}{c}$ , which is the two-way doppler frequency. Therefore, the entire spectrum has been translated in frequency by this amount. In addition to  $f_d$  each spectral component contains its spectral frequency doppler shift. Since each spectral component occurs at a slightly different RF frequency, these doppler shifts are not equal in magnitude. Therefore, the component  $\frac{f_c}{11}$  away from the S-band carrier



will be translated an additional  $f_{d1} = \left[ \frac{2v_s}{c} \right] \left[ \frac{f_c}{11} \right]$  the component at  $\frac{3f_c}{11}$  will be translated an additional  $f_{d2} = \left[ \frac{2v_s}{c} \right] \left[ \frac{3f_c}{11} \right]$ , and so on for each spectral component. The clock component then will be shifted by  $f_{dc} = \frac{2v_s}{c} f_c$  in addition to the doppler component  $f_d$ . These characteristics are shown in the spectrum of figure 2.

Now let us consider the generalized case. The effective doppler velocity, which is the radial component of velocity between the spacecraft and ground station, will vary with time. The rate and magnitude of this variation is a function of such parameters as the spacecraft's instantaneous position with respect to the ground station, and the earth's rotational velocity. The effects of this will be to smear the returned spectrum; that is, the doppler frequencies will vary with time, proportional to the variations in radial velocity. Therefore, the returned spectrum will be different at any instant of time depending on the instantaneous doppler frequency.

The returned signal will also be delayed in time by an amount proportional to the spacecraft's range. Since the power spectrum of a periodic function is not dependent on the phase angles of its harmonics, the time delay which effectively introduces a phase shift does not alter the received power spectrum as seen in figure 2. However, the ranging system must extract this time delay or phase information for measurement of initial range. Therefore, it is of interest to consider the transmitted and returned signals in the time domain, and the technique for making the actual range measurement. Since the transmitter code,  $C(t)$ , is phase modulated onto the RF (S-band) carrier, we can designate the transmitted signal as  $f[C(t)]$ . Then the received signal will be delayed in time by an amount  $\tau_c$ , depending on the spacecraft's range. Thus the received signal can be designated  $f[C(t + \tau_c)]$ . In the ranging system the received signal is multiplied by a logically programed sequence of subcode combinations. This multiplication yields a correlation function. The receiver subcodes bits<sup>2</sup> are then shifted one bit at a time until a maximum correlation is obtained for each program state. The entire code shift is determined from the individual subcode shifts by application of the Chinese remainder theorem. The total phase shift of the received code is a measure of the round trip time delay  $\tau_c$ , and hence a measure of range at time zero.

As the spacecraft moves away from the ground station, the range time varies as a function of the velocity. This produces the doppler

$f_c$  = Transmitter Carrier

$f_1$  = S-Band Carrier

$$\frac{1}{T} = 2f_c$$

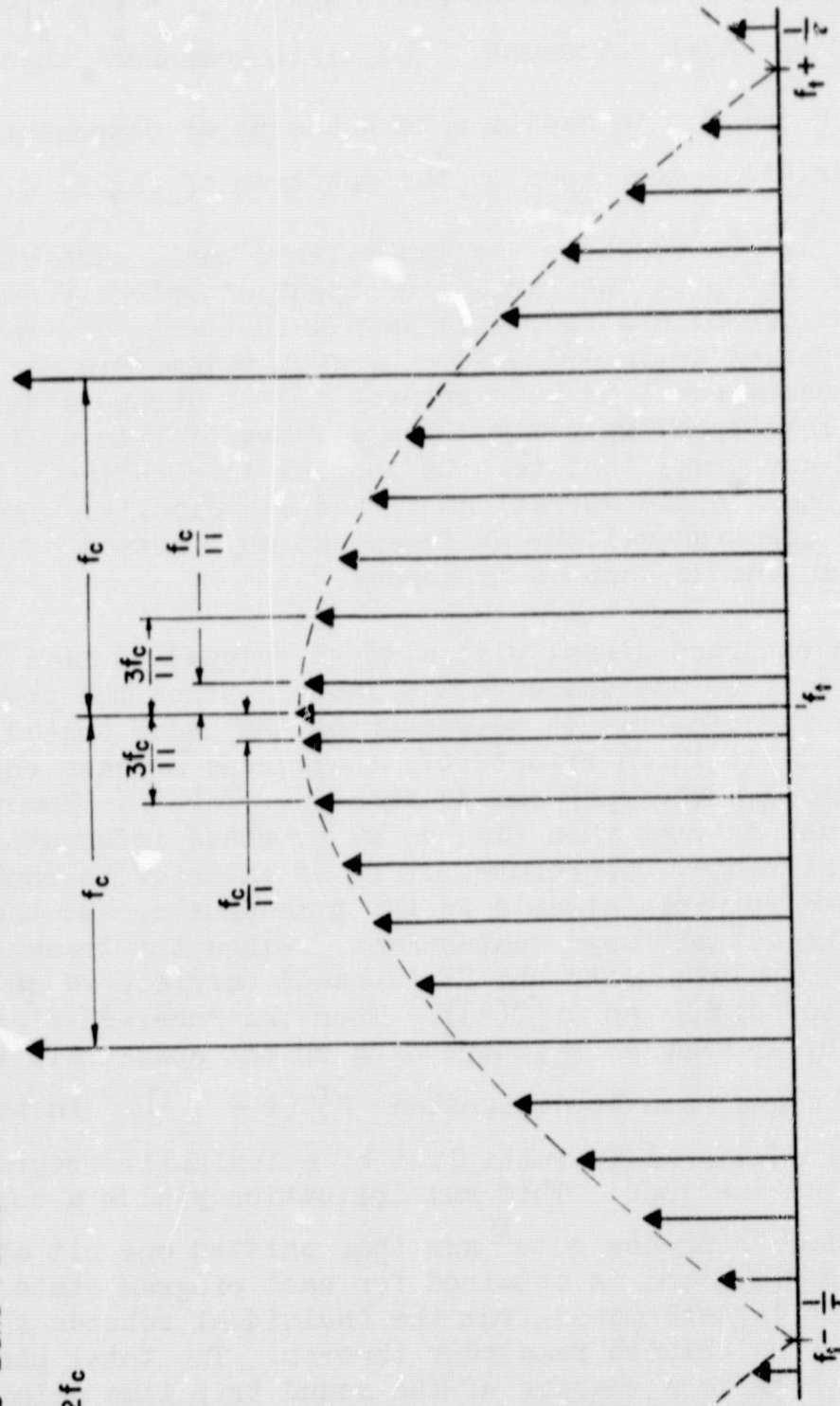


Figure 1.  
TRANSMITTED RF SPECTRUM



$$f_d = \frac{2v_s}{c} f_t$$

$$f_{dc} = \frac{2v_s}{c} f_c$$

$$f_{d1} = \left[ \frac{2v_s}{c} \right] \left[ \frac{f_c}{11} \right]$$

$$f_{d2} = \left[ \frac{2v_s}{c} \right] \left[ \frac{3f_c}{11} \right]$$

$$\frac{1}{T} = 2f_c - \frac{4v_s}{c} f_c$$

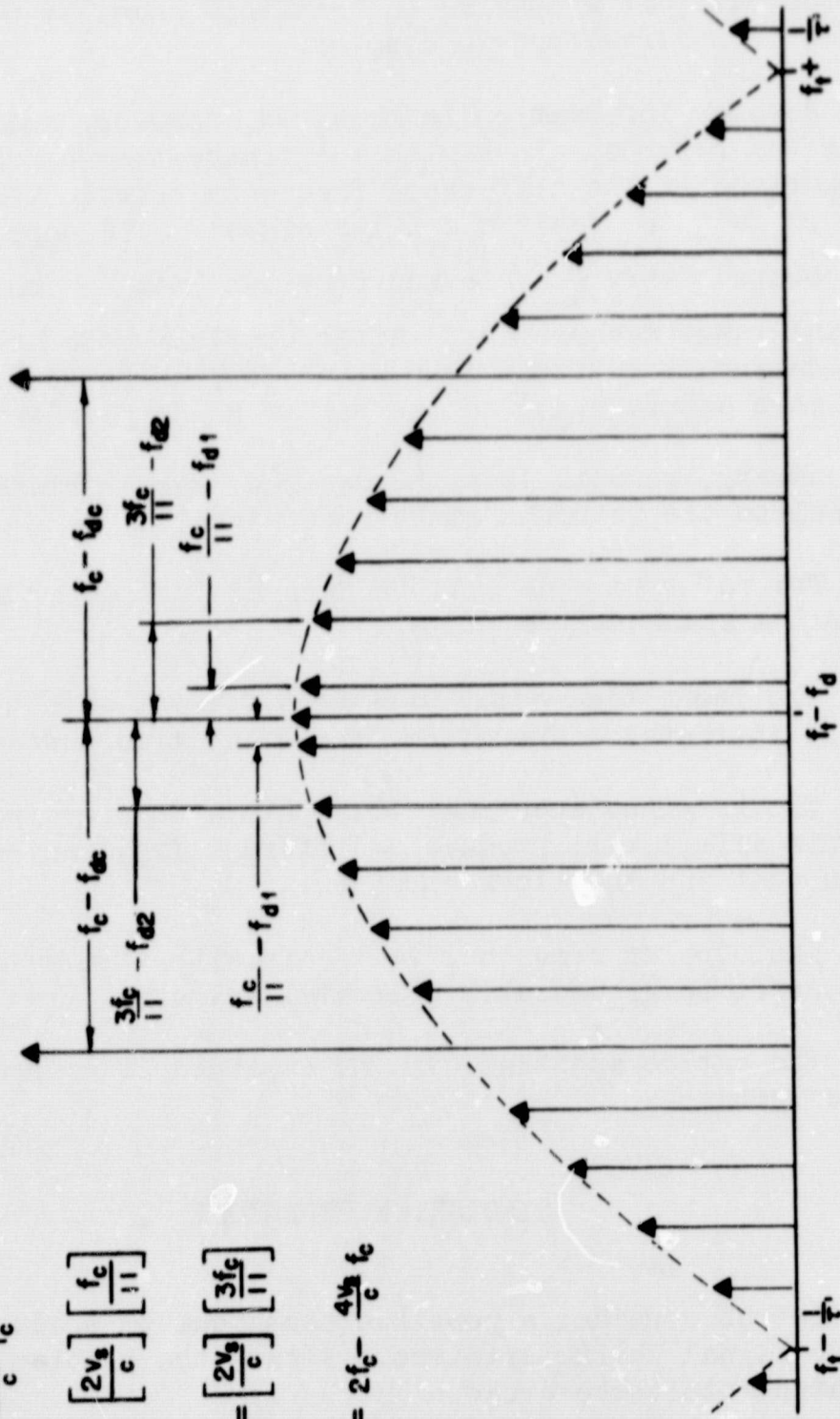


Figure 2.  
RECEIVED RF SPECTRUM

phenomenon discussed earlier. In the range code acquisition loop the doppler effect is essentially canceled. This is achieved by slaving the receiver code generator to the returned clock signal which contains the doppler information. Thus, the receiver code runs at the same rate and has the same bit widths as the returned code, so no phase shifts or delay time is observed due to doppler.

The doppler information is required, however, and is obtained by comparing the returned clock with the transmitter clock. The result of this comparison is the difference frequency between these two signals which is in fact the desired doppler signal. The doppler information is then counted every  $\frac{1}{4}$  cycle and provides data to continuously up-date the initial range measurement. After complete code acquisition, the range up-dating is switched from clock doppler to RF doppler. This provides more accuracy due to the higher RF doppler frequency.

In summary, we will list the desired characteristics to realistically simulate the returned range code signal.

1. The returned code must be delayed in time by an amount proportional to the spacecraft's range.
2. The range time delay will be different each time the acquisition process is initiated. Therefore, the delay time must be variable.
3. The returned spectrum will contain doppler frequency information. This effect will produce a different frequency shift on each spectral component and the clock component.
4. The doppler frequency will vary with time as a function of the spacecraft to ground station radial velocity.
5. The entire spectrum will be expanded or compressed due to the doppler effects.

#### SIMULATION TECHNIQUE

Now let us consider a possible technique to produce the desired range code signal characteristics. First, the problem may be simplified if separated into three areas.

1. RF doppler simulation.



2. Code doppler simulation.

3. Range time delay.

A discussion of each of these areas follows.

### RF Doppler Simulation

To produce the RF doppler component  $f_d$  in the received spectrum, a stable voltage controlled oscillator and frequency translation system is required. A block diagram of such a system is shown in figure 3. To provide a phase coherent signal a portion of the transmitter master VCO is coupled from the ground system to the simulator. This signal is fed to an isolation and distribution amplifier which provides three outputs at the master VCO frequency which is denoted  $f_o$ . One of the signals is divided in frequency by 16 yielding  $\frac{f_o}{16}$ , and then mixed with a second output of the isolation amplifier. By incorporating a balanced mixer, the carrier is suppressed and two side bands are produced. The upper side band is selected by filtering which provides a signal whose frequency is  $\frac{17}{16} f_o$ .

The third output of the isolation amplifier is mixed with the S-band transmitter signal  $f_t$ , which is obtained from the ground station RF circuitry. The output of this mixer is filtered to select the lower side band component  $(f_t - f_o)$ . To produce the desired amount of doppler shift a stable voltage-controlled oscillator, which is centered nominally at a frequency of  $\frac{f_o}{16}$ , is controlled by a doppler analog signal. This signal drives the oscillator to a frequency of  $\left(\frac{f_o}{16} + f_d\right)$  to simulate the RF doppler shift. The  $f_d$  then varies proportionally to the doppler control signal. The output of the VCO  $\left(\frac{f_o}{16} + f_d\right)$  is mixed with the  $\frac{17}{16} f_o$  signal and the lower side band  $(f_o - f_d)$  is selected by filtering. Notice here that a frequency inversion is obtained due to selecting the lower side band. Thus a negative doppler, as desired for simulating an opening velocity, is obtained. Either opening or closing doppler shifts may be obtained depending on the sign of the frequency shift at the VCO. The filtered output signal  $(f_o - f_d)$  is then mixed with the

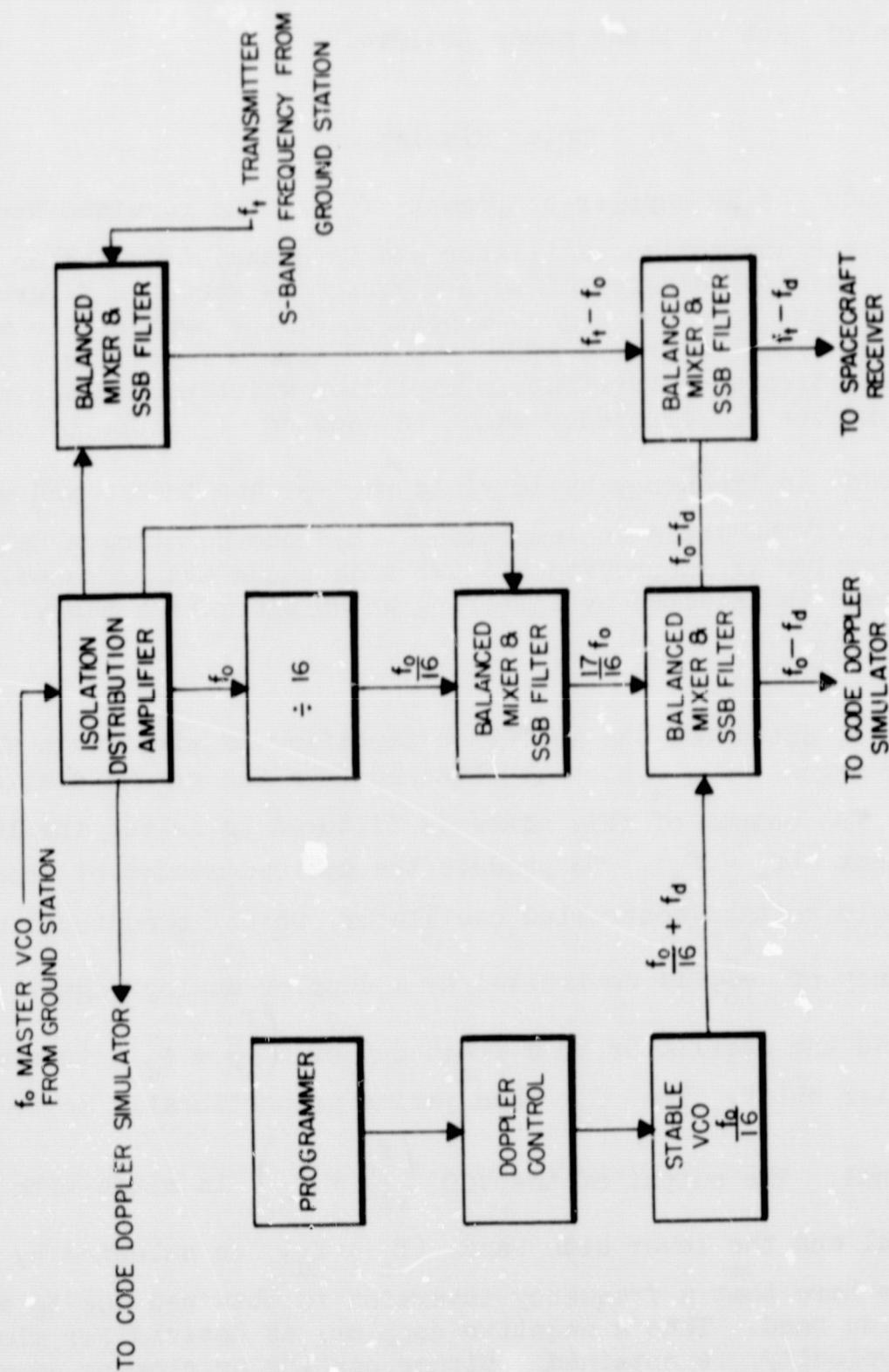


Figure 3.  
RF DOPPLER SIMULATOR



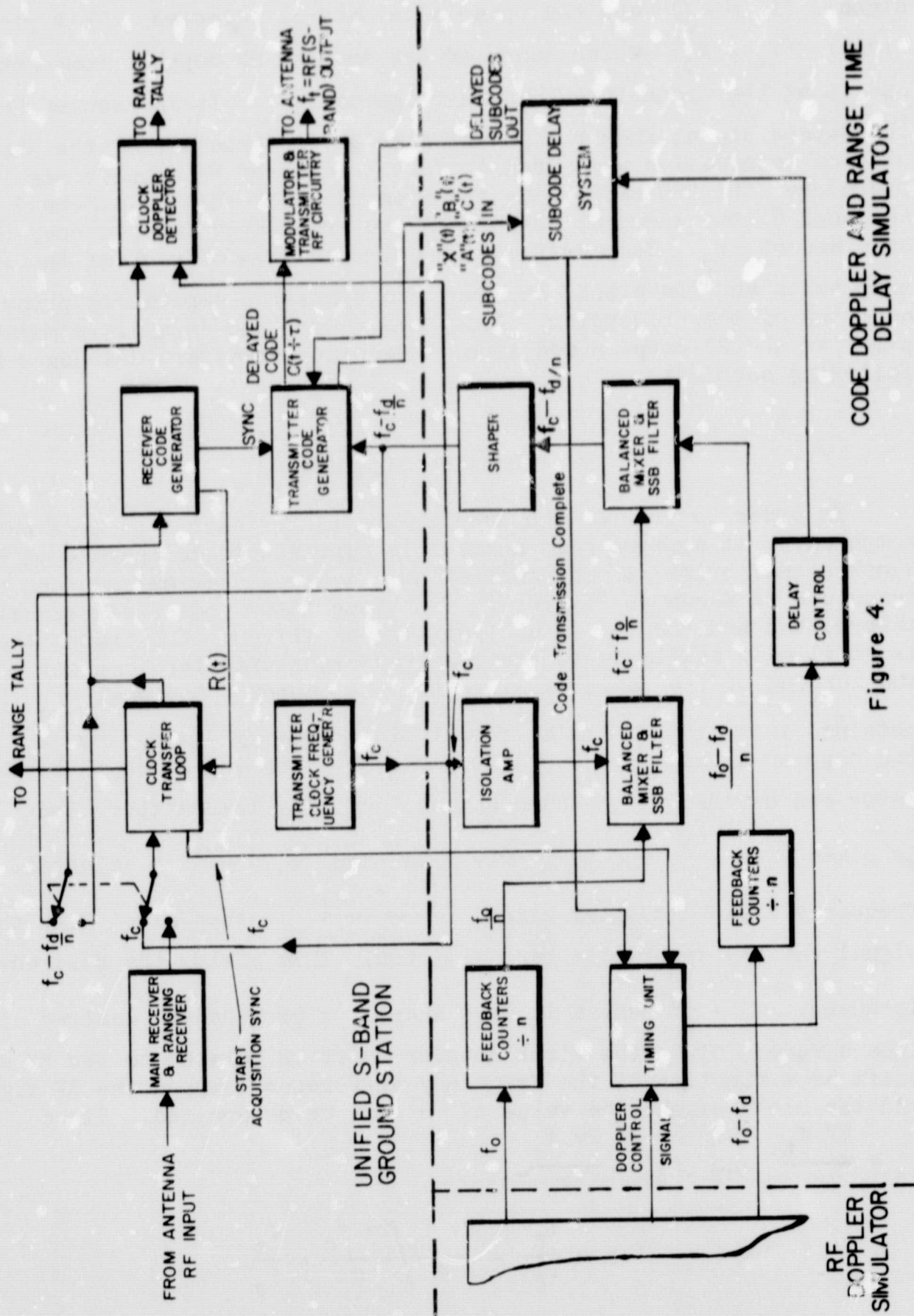
signal  $(f_t - f_o)$  and the upper side band is selected. This yields the signal  $(f_t - f_d)$  which contains the desired RF doppler component  $f_d$  and is at the transmitter S-band frequency  $f_t$ . It is assumed here that the S-band signal from the ground station contains all of the phase modulation information when used in this process of RF doppler simulation. Therefore, the PRN range code spectrum is centered at the S-band carrier and each of the spectral components are translated in frequency by the same amount  $f_d$ . The additional doppler shifts for each of the spectral components and the clock component are simulated separately prior to the addition of the RF doppler. Also, the range time delay is simulated prior to the RF doppler addition. These processes are discussed in the following sections.

#### Code Doppler Simulation

In order to provide the doppler shifts for each subcode's spectral components, it appears that a feasible approach is to operate on the clock signal prior to code generation. A block diagram for such a technique is shown in figure 4. The transmitter code clock signal is interrupted and coupled to an isolation amplifier. The transmitter clock is still made available to the receiver clock transfer loop for clearing and zeroing of the range tally unit. The master VCO signal  $f_o$  is obtained from the RF simulator unit and frequency divided by  $n$ . Also, the doppler signal  $(f_o - f_d)$  is obtained from the RF doppler simulator and divided by the same amount,  $n$ . The transmitter clock  $f_c$  is mixed with  $\frac{f_o}{n}$  and the lower side band  $f_c - \frac{f_o}{n}$  is selected. The frequency divided doppler signal  $\frac{(f_o - f_d)}{n}$  is then mixed with this signal and the upper side band selected. This yields the desired clock frequency  $f_c - \frac{f_d}{n}$  which is then shaped to provide the desired clock square wave. Since the clock doppler shift is related to the RF doppler shift as a function of the frequency difference between the RF signal and the clock signal the value of  $n$  can be determined. Since

$$f_d = \frac{2v f_t}{c} \quad \text{and} \quad f_{dc} = \frac{2v f_c}{c}$$

$$n = \frac{f_d}{f_{dc}} = \frac{2v f_t / c}{2v f_c / c} = \frac{f_t}{f_c}$$





$$n \approx \frac{2000 \times 10^6}{500 \times 10^3} \approx 4000$$

There are several apparent advantages to deriving the clock doppler directly from the RF doppler signal.

1. The RF and clock doppler must be phase coherent which is insured by this technique.

2. The clock doppler and RF doppler always vary as a direct ratio of their frequencies, i.e.,  $\frac{f_c}{f_t} = \frac{1}{n}$ .

3. The rate of variations in clock and RF doppler is identical, which will be insured by this technique.

4. A single doppler control and VCO system can provide both of the doppler signals.

When the transmitter code generator is operated from the nominal clock frequency  $f_c$ , an RF spectrum as shown in figure 1 is produced. Since

the clock frequency is now shifted by an amount  $f_{dc} = \frac{f_d}{n}$  the RF spectrum will appear as shown in figure 5. Therefore, it is seen that a change in clock frequency by an amount  $f_{dc}$  produces a code spectrum in which each spectral component is shifted in frequency by the desired amount. When the RF doppler is added to this S-band spectrum, the entire spectrum shown in figure 5 is shifted in frequency by  $f_d$ . This process will then provide a spectrum as shown in figure 2. Thus operating on the code clock prior to generation of the code signal provides a realistic simulation of the returned spectrum. Since an effect of this doppler shift is to compress or expand the entire spectrum, it is of interest to show that this condition is obtained by varying the clock signal. To illustrate this phenomenon figure 6 shows the code spectrum

envelope  $\left(\frac{\sin X}{X}\right)^2$  for the nominal clock rate. It is seen that the nulls occur at  $\frac{1}{\tau}$  where  $\tau$  is the bit width. In the code generator the clock signal, which is nominally a square wave of period  $T = \frac{1}{f_c}$ , is operated on to provide the code generating pulses. This is shown in figure 7A and B. Thus it is seen that the bit width  $= \frac{T}{2}$  for the

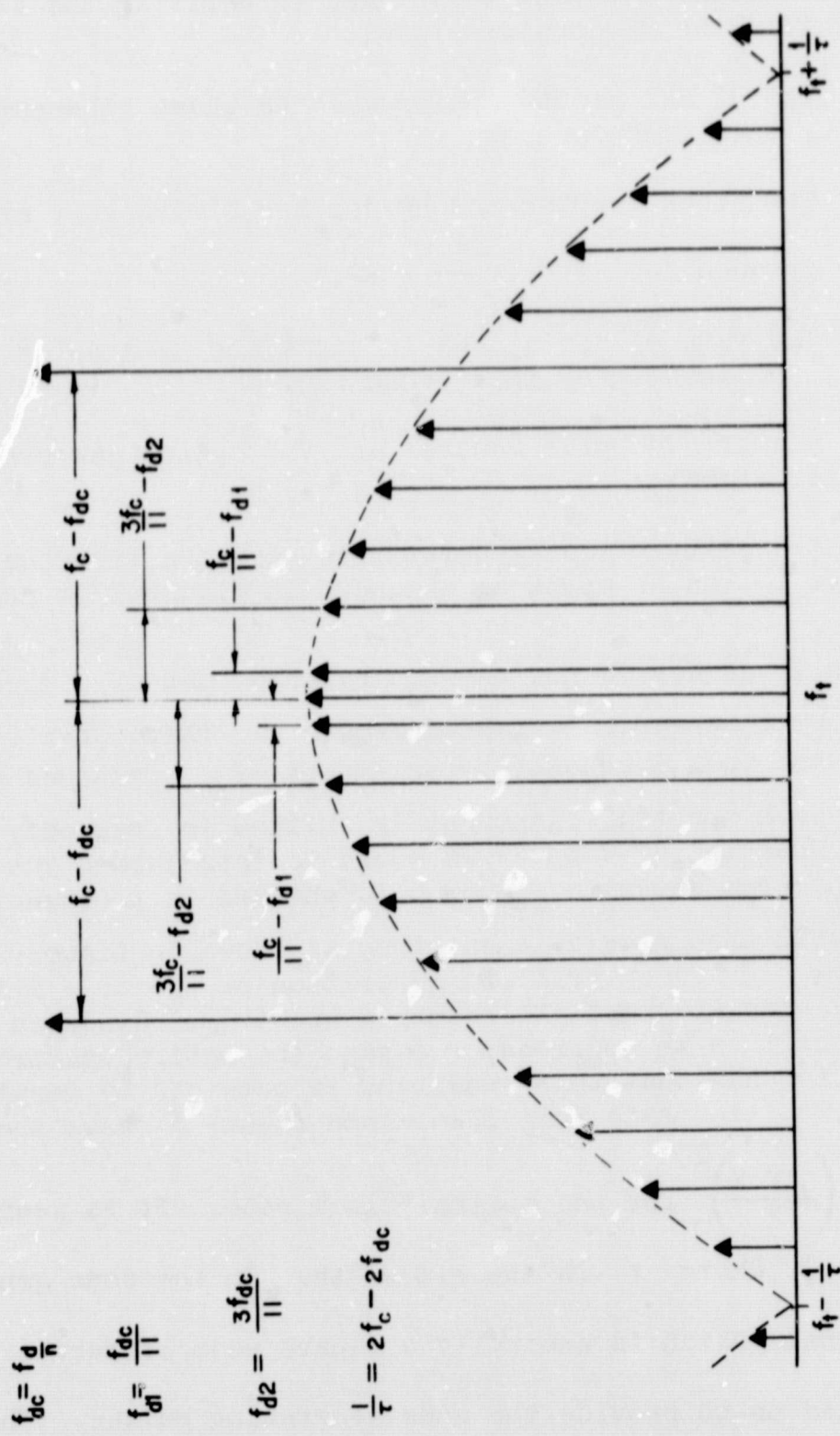


Figure 5.  
RF CODE / SPECTRUM WITH CLOCK DOPPLER

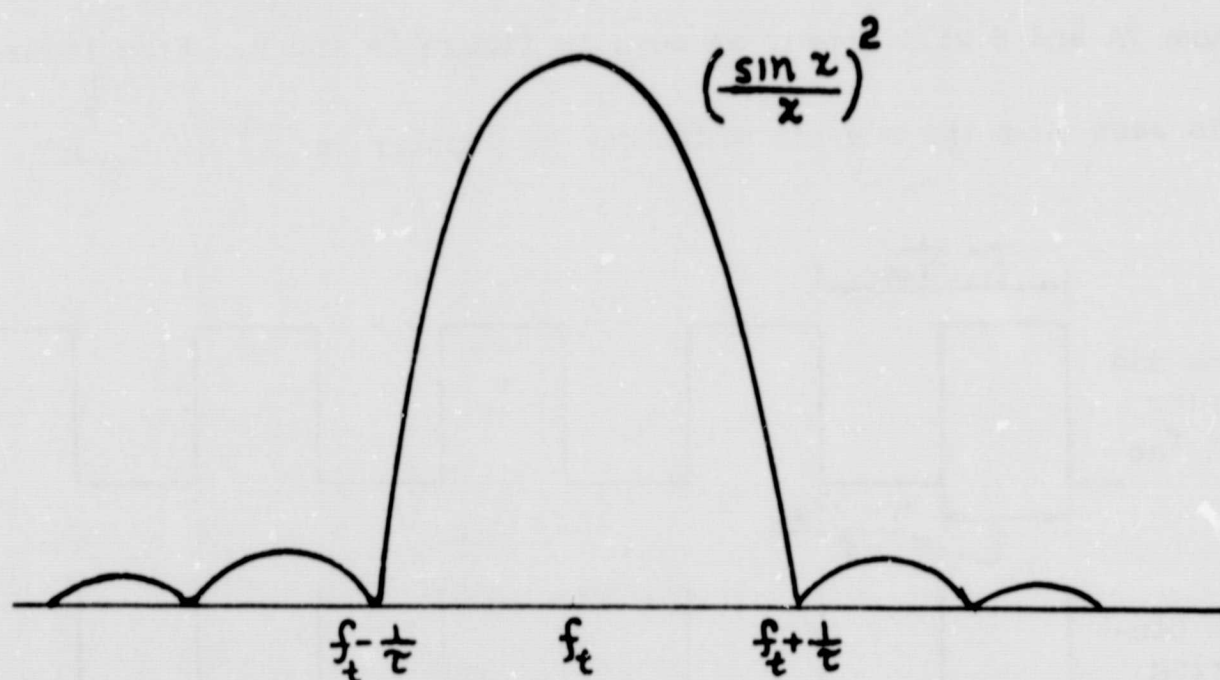


Figure 6

nominal case. When the clock doppler is added, the clock period  $T$  increases or decreases by an amount  $\frac{1}{f_{dc}}$ . Now the wave forms shown in

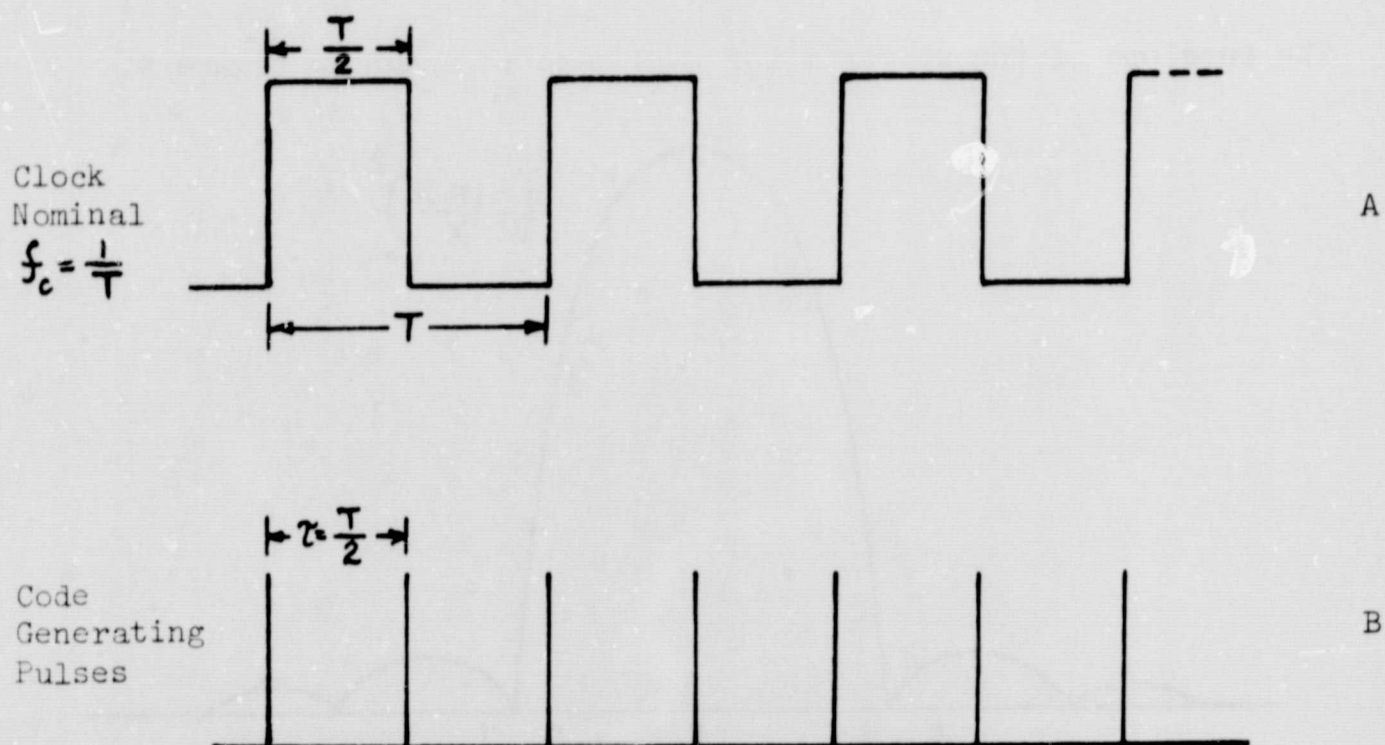


Figure 7



figure 7A and B will appear as seen in figure 8A and B. From figure 8B it is seen that the new bit width due to doppler is  $\tau^1 = \frac{T - \frac{1}{f_{dc}}}{2}$

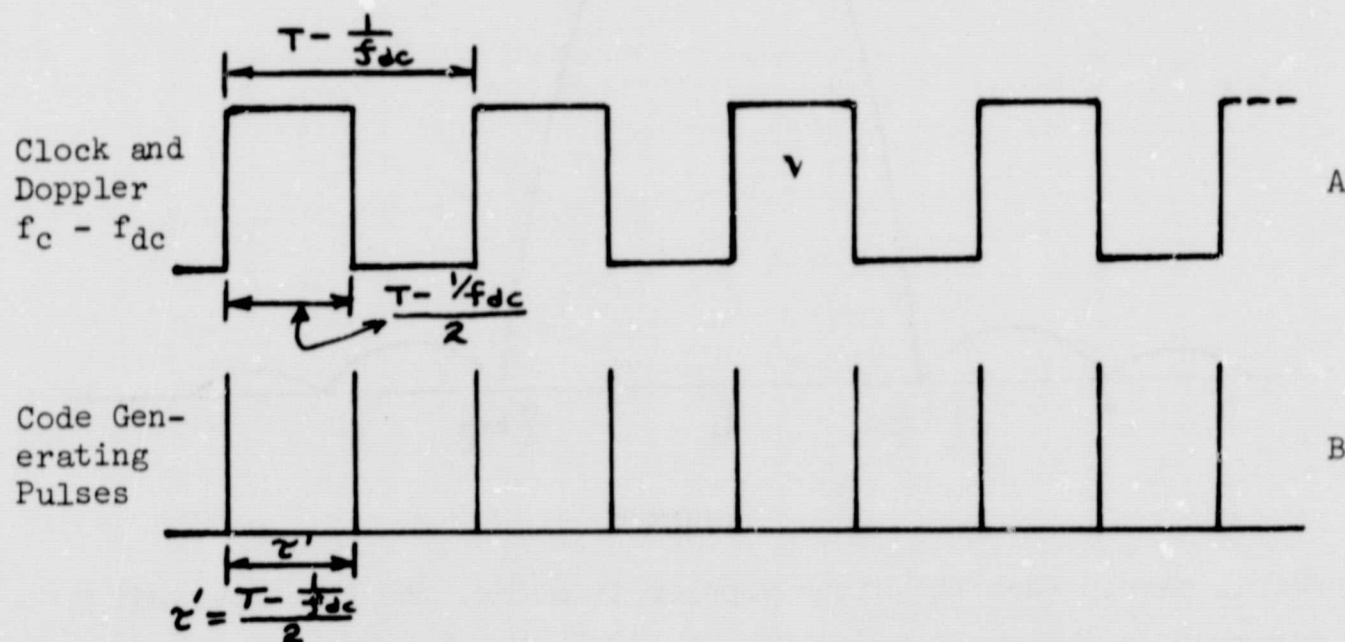


Figure 8

The envelope of the spectrum for this case is shown in figure 9.

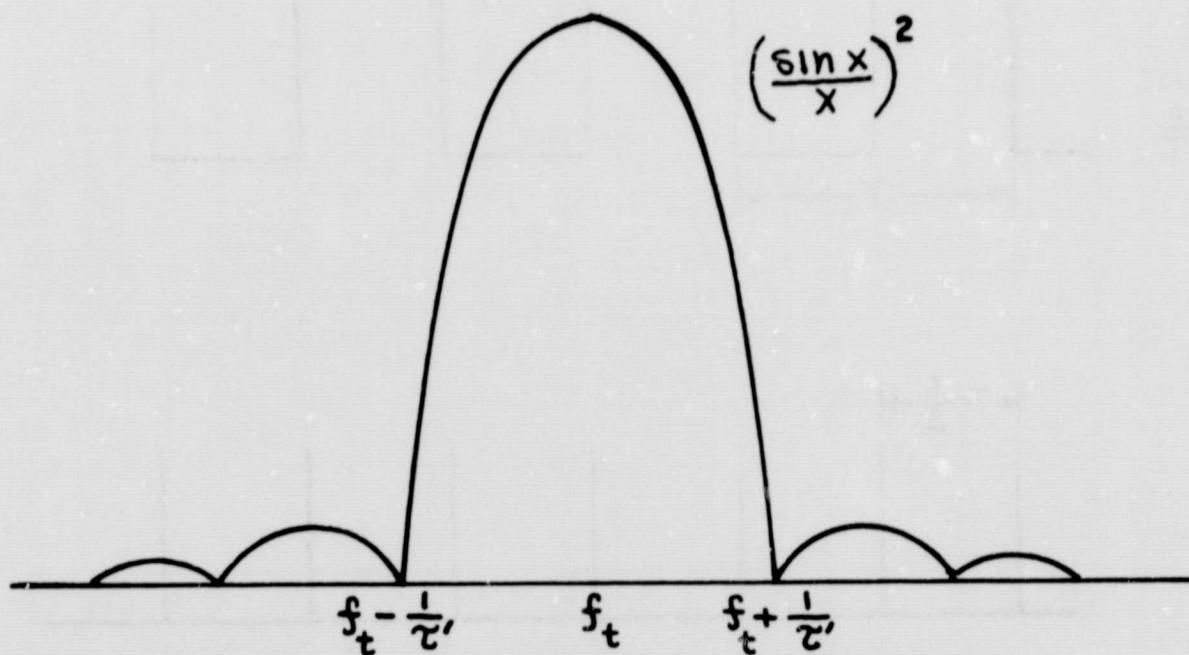


Figure 9

Let us now summarize the results obtained by this technique of simulation.

1. Each of the subcode's spectral components are shifted in frequency by an amount proportional to their respective frequencies, i.e., the  $\frac{1}{11} \times f_c$  component is shifted by  $\frac{f_{dc}}{11}$ , the  $\frac{3}{11} f_c$  component is shifted by  $\frac{3 f_{dc}}{11}$ , etc.

2. The bit width varies proportional to the doppler  $f_{dc}$ . Thus the entire spectrum is expanded or compressed.

3. The clock doppler is phase coherent with the RF doppler. Therefore, variations in the RF doppler signal are precisely reproduced in the clock doppler signal.

4. The clock doppler can be precisely maintained at the ratio of clock to RF frequencies  $\frac{1}{n} \approx \frac{1}{4000}$ .

5. The doppler signals are phase coherent with the transmitter clock since they are derived from the same master VCO.

#### Range Time Delay

Let us now consider the final phase of simulation. A time delay must be imparted to the transmitter code before it is returned to the ground station receiver. At lunar distance the round trip delay will approach three seconds. Each time the range code acquisition is initiated the time delay is different due to spacecraft velocity. Thus a variable delay time is desired. Due to the signal characteristics and the magnitude of the delay, conventional techniques are inadequate. However, it appears feasible that such a delay might be obtained using delay lines or digital techniques and operating on the individual subcode elements. A discussion of a technique, using delay lines, as shown in figures 4 and 10 follows. Upon initiation of the ranging process each of the subcodes are coupled from the transmitter code generator to the delay system. The subcodes are delayed in individual tapped delay lines, the appropriate number of microseconds to simulate the entire code delay desired. The delay lines will be tapped each microsecond to allow selecting any number of bit delays from zero (0) to the entire number of bits in the subcode element. For example, the X component will pass through an eleven (11) microsecond delay line with taps at



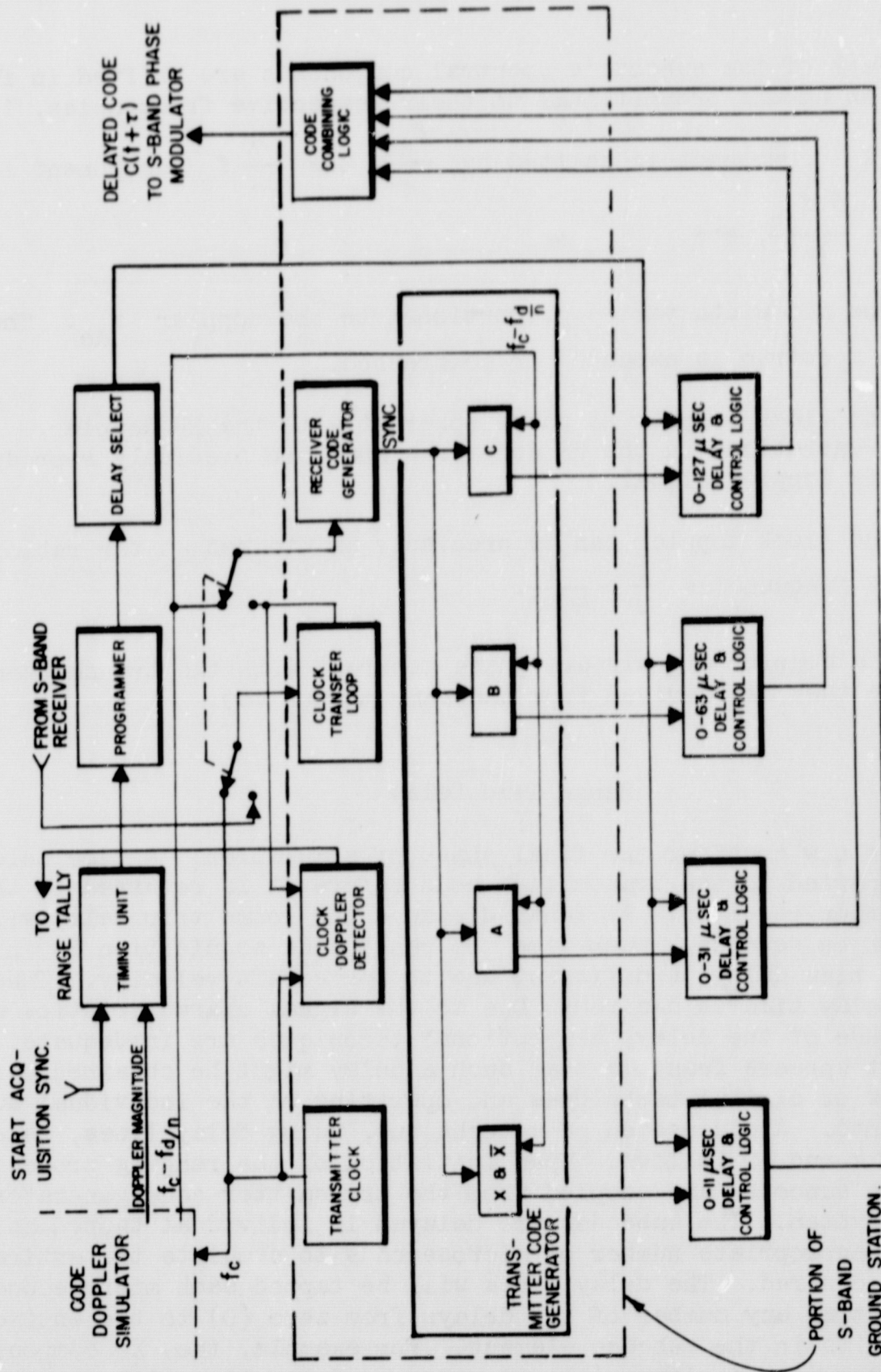


Figure 10.  
RANGE TIME DELAY SYSTEM



1, 2, ..... 11 microseconds. The tap selected is dependent upon the total code delay that is to be simulated.

Now assume that it is desired to simulate a range time delay of .75 seconds. The time delay for each subcomponent will be as shown below.<sup>2</sup>

Time delay of "X" component 9 bits = 9 microseconds

Time delay of "A" component 19 bits = 19 microseconds

Time delay of "B" component 48 bits = 48 microseconds

Time delay of "C" component 65 bits = 65 microseconds

Therefore, delaying each of the subcodes the amount indicated above, and then logically combining these delayed components into the combined code, will simulate the desired time delay of .75 seconds for the combined code.

Since the receiver and transmitter code generator must be synchronized during state P2 of the receiver programed states, both the transmitter and receiver code generator must operate from the shifted clock signal, i.e.,  $\left(f_c - \frac{f_d}{n}\right)$ . During this state it is also necessary to reset the range tally to zero. This requires that the transmitter clock reference to the clock doppler detector and the transfer loop VCO be identical in frequency.

Since the transfer loop is initially locked to the transmitter clock, this provides zero doppler from the clock doppler extractor. However, since the transmitter code generator is running at the (clock-clock doppler) rate, it is necessary to provide a means for synchronizing the receiver and transmitter code generators. This is done by switching the receiver code generator clock input from the transfer loop VCO to the  $(f_c - f_{dc})$  signal.

The last operation in state P2 is to connect the clock transfer loop to the receiver clock. At this time the receiver code generator clock input is switched back to the transfer loop VCO, and counting of clock doppler begins.

For automatic operation a timing unit can sense the doppler being simulated and supply a signal to the subcode delay programmer to change the various delays the appropriate amount. The timing system can be

synchronized with the start acquisition signal to provide the proper delay each time the ranging process is initiated.

We have now provided the required time delay and doppler shifts to realistically simulate the returned signal.

### CONCLUSIONS

Based on present knowledge it appears that realistic simulation of doppler and range time delay can be accomplished. However, this will require sophisticated special test equipment. The cost of such equipment must be considered with respect to the additional capabilities and confidence which would be obtained. Such a simulation system might accomplish:

1. The confidence which can be provided by a test program, such as that undertaken by MSC/ISD, is entirely dependent upon the realism which can be accomplished in simulating actual flight parameters. This fact alone makes dynamic spacecraft simulation extremely desirable.
2. The entire ranging system can be completely exercised. This will allow verification of all pertinent parameters, such as accuracy, acquisition time, doppler thresholds, loop tracking capabilities, effects of loss of lock, etc.
3. The effects of the data and communication channels on the system's ability to accurately extract and measure doppler can be verified.
4. The capability of the receiver to acquire the doppler shifted carrier and its ability to track the signal for realistic doppler rates can be verified.
5. The effects of carrier doppler variations on information and communication channels can be studied and verified.
6. The capability of the ranging system to acquire after loss of lock and provide the correct range data can be verified.
7. Dynamic spacecraft simulation provides a means for realistically simulating missions. This can provide valuable training and experience for flight operations personnel.
8. To effectively verify compatibility and accuracy of data transfer between remote-site ground stations and IMCC, realistic simulation of such data is extremely desirable.

9. It appears that such a simulation technique could be extended to include shifting of information subcarriers, and data rates to effectively simulate doppler effects on the information handling capability of the system. However, additional investigation in this area will be necessary.

10. Due to frequency limitations of the USB transponder up and down link doppler will have to be simulated separately. This would require an additional RF doppler simulator for use with the spacecraft output signal.

#### REFERENCES

1. Apollo Unified S-Band System Test Phase I, Volume I and II, Motorola Inc., Military Electronics Division.
2. Apollo Pseudo Random Noise Ranging System, NASA/MSC; Jan W. Martin, ISD, July 6, 1964.
3. The Apollo Unified S-Band Telecommunication System, Volume I, NASA/MSC, John H. Painter and George Hondros, ISD.
4. Technical Report No. 32-67 Coding Theory and Its Applications to Communication Systems, Jet Propulsion Laboratory, March 31, 1961.
5. Statistical Theory of Communication, Lee, Y. W. (John Wiley and Sons, Inc., New York, New York, 1960).



## APPENDIX

For the practical case, it has been shown that the range code can be represented in the time domain as a Fourier series expansion of the form:

$$r(t) = \sum_{j=1}^{\infty} b_j \cos(\omega_j t + \theta_1)$$

$$\omega_j = \frac{2n\pi}{11} f_{CL} \quad \text{where } j = n$$

setting the arbitrary phase angle  $\theta_1$  to zero

$$r(t) = \sum_{j=1}^{\infty} b_j \cos \omega_j t$$

The signal  $r(t)$  is then phase modulated on the S-band carrier frequency,  $f_o$ , yielding the expression

$$f_T(t) = A_o \cos \left[ \omega_o t + \sum_{j=1}^{\infty} b_j \cos \omega_j t \right]$$

Taking only  $k$  terms for the Fourier series expansion of the range code

$$f_T(t) = A_o \cos \left[ \omega_o t + \sum_{j=1}^k b_j \cos \omega_j t \right]$$

such that

$$\frac{k}{11} f_{CL} \geq 3f_{CL}$$

or

$$k \geq 33 (k \text{ odd})$$

$f_T(t)$  can be expanded to

$$f_T(t) = A_o \sum_{n_1=-\infty}^{\infty} \sum_{n_2=-\infty}^{\infty} \dots \sum_{n_k=-\infty}^{\infty} J_{n_1}(b_1) \dots J_{n_k}(b_k) \cos \left[ (\omega_o + \sum_{j=1}^k n_j \omega_j) t \right] \quad (1)$$

This signal is transmitted to a spacecraft moving at a radial velocity, relative to the ground station, of  $v_r$ . Therefore the received signal will be of the form

$$f_R(t) = A_0 K \sum_{n_1=-\infty}^{\infty} \sum_{n_2=-\infty}^{\infty} \dots \sum_{n_k=-\infty}^{\infty} J_{n_1}(b_1) \dots J_{n_k}(b_k) \cos \left[ \left( \omega_0 + \sum_{j=1}^k n_j \omega_j + \omega_d \right) (t - T) \right] \quad (2)$$

where  $T = \frac{2R}{c}$   $K = \text{attenuation constant}$   $R = \text{range}$

$$\text{and } \omega_d = \frac{2v_r}{c} \left[ \omega_0 + \sum_{j=1}^k n_j \omega_j \right] = D \left[ \omega_0 + \sum_{j=1}^k n_j \omega_j \right]$$

where  $D$  is used to denote the doppler constant assuming a constant velocity spacecraft.

Equation (2) can be rewritten as

$$f_R(t) = A_0 K \sum_{n_1=-\infty}^{\infty} \sum_{n_2=-\infty}^{\infty} \dots \sum_{n_k=-\infty}^{\infty} J_{n_1}(b_1) \dots J_{n_k}(b_k) \cos \left\{ \left[ (1 + D) \omega_0 + (1 + D) \sum_{j=1}^k n_j \omega_j \right] (t - T) \right\} \quad (3)$$

Equation (3) shows that both the carrier frequency,  $f_0$ , and each frequency of the range code, is multiplied by the factor  $(1 + D)$ , and that the modulated spectrum is symmetrical about  $(1 + D)\omega_0$ . Since the received base band code spectrum is derived by means of coherent demodulation, the process of "folding over" the lower side band on to the upper side band appears to be no problem.

The effect of the factor  $(1 + D)$  on the range code clock signal is to shorten the bit width of the code components. That is to say, originally the bit period of the code components was equal to

$$T_t = \frac{1}{2f_{CL}} \quad \text{the bit width period of the received code components is}$$

$$T_R = \frac{1}{2f_{CL}(1 + D)} \quad \text{Since the receiver code generator is driven by}$$

pulses which are coherently related to the received clock signal, the problem of matching bit widths of received code and receiver code does not arise.

Suppose now that instead of transmitting the signal  $f_T(t)$  of equation (1), some modifications were made on the carrier frequency,  $f_o$ , and the transmitter code generator sync pulses. That is, let,

$$\omega_c = (1 + D)\omega_o$$

and

$$\omega_{CL} = (1 + D)\omega_{CL}$$

$r(t)$  would now equal

$$r_1(t) = \sum_{j=1}^{\infty} b_j \cos \left[ (1 + D)\omega_j t' + \theta_i \right]$$

$$r_1(t) = \sum_{j=1}^k b_j \cos \left[ (1 + D)\omega_j t' \right] \text{ for } k \text{ summations } \theta_i = 0^\circ$$

Phase modulating the carrier with this modified signal results in

$$f(t) = A \cos \left[ \omega_c t' + \sum_{j=1}^k b_j \cos (1 + D)\omega_j t' \right] \quad (4)$$

Expanding (4) yields

$$f(t) = A \sum_{n_1=-\infty}^{\infty} \sum_{n_2=-\infty}^{\infty} \dots \sum_{n_k=-\infty}^{\infty} J_{n_1}(b_1) \dots J_{n_k}(b_k) \cos \left[ \omega_c t' + \sum_{j=1}^k n_j (1 + D)\omega_j t' \right]$$

Substituting  $(1 + D)\omega_o = \omega_c$

$$f(t) = A \sum_{n_1=-\infty}^{\infty} \sum_{n_2=-\infty}^{\infty} \dots \sum_{n_k=-\infty}^{\infty} J_{n_1}(b_1) \dots J_{n_k}(b_k) \cos \left[ (1 + D)\omega_o t' + \sum_{j=1}^k n_j (1 + D)\omega_j t' \right] \quad (5)$$

Equation (5) is identical to equation (3) for the substitution  $t' = t - T$ . Therefore it appears possible that RF doppler and range code doppler simulation can be achieved by methods proposed in this paper.